Nonlinearities in bismuth under supersonic electron drift

Yu. A. Bogod
Department of Condensed Matter Physics, The Weizmann Institute of Science, 76100 Rehovot, Israel

P. Finkel
Department of Physics, Queens College of The City University of New York, Flushing, New York 11367
(Received 23 May 1994; revised manuscript received 17 January 1995)

The transverse voltage $V_\perp$ of a homogeneous, high-purity bismuth sample in strong crossed electric and magnetic fields in the phonon-generation regime was studied. A method of directly determining the acousto emf E^a from the I-$V_\perp$ characteristics has been developed. It is shown that in the nonlinear regime the I-$V_\perp$ curves contain parts with a negative differential conductivity. Nonreciprocity of the nonlinear transverse voltage was found when the magnetic field or current directions are reversed. This is related to different degrees of phonon damping on opposite transverse sample faces as well as a contribution from a component of $V_\perp$ that is even in H. Several peculiarities were found in $V_\perp$ that are familiar from studies of the longitudinal component of the nonlinear voltage, namely, electroacoustic oscillations, relaxation rate dependence on H, and "aftersound." Under certain conditions the electroacoustic oscillations of $V_\perp$ were transformed into noise, marking the presence of acoustic turbulence and the onset of chaos. At high values of the electron drift velocity, the differential conductivity abruptly changes sign. This is explained in terms of a radical increase in the nonlinear phonon-phonon damping, causing a decrease in the nonequilibrium phonon concentration.

INTRODUCTION

The effects of elastic wave amplification of supersonic drifting electrons were first observed in piezosemiconductor crystals of CdS.[1] In 1962–1963 (Ref. 2), it was discovered that Bi in the presence of a magnetic field exhibits the generation of acoustic noise accompanied by a kink in the I-V curve that is followed by a regime of increased conductivity (the Esaki effect).[3]

Since then, Bi remains the only metallic substance where the generation of nonequilibrium phonons in the bulk has been observed experimentally.[4–6] The remarkable feature of Bi is that the threshold current density sufficient for the charge carriers' drift velocity to exceed the acoustic wave velocity is relatively small. For typical metals, these values are of the order of 10^9 A/cm^2, while for Bi it is on the order of $10-10^3$ A/cm^2. This large contrast is a result of the lower carrier concentration and smaller cyclotron mass in Bi.

Thus, the necessity to attain high current densities presents a major technical obstacle to the experimental study of typical metals in the phonon-generation mode. The low-heat capacity of most metal samples causes sample heating at low temperatures, making it difficult to reach the critical current density. Another experimental difficulty is that the current pulse heats the sample in a time short compared to the characteristic relaxation time to enter the phonon-generation regime; this makes it difficult to differentiate the thermal effects from the acoustic ones.

The Esaki effect is observed in crossed electric and magnetic fields when the carriers drift with a supersonic velocity $\mathbf{v}_\perp^d \cong cE/H > s$ in the direction perpendicular to the current flow; s is the speed of sound in the material. This effect takes place at current densities $j > j_k = nes/\Omega\tau$ with $\Omega\tau \gg 1$, where $\Omega = eH/m^*c$ is the cyclotron frequency and τ is the momentum relaxation time. A kink in the I-V curves toward increasing resistance caused by longitudinal phonon generation in the bulk was observed in 1983 in filamentous crystals of Bi of thickness 3 μm at $H=0$ and at current densities $j > nes$.[7] A similar kink preceding the Esaki effect was observed in 1986 in filamentous 1–10-μm Bi crystals in strong crossed electric and magnetic fields.[8] This phenomenon occurs at average current densities $\langle j \rangle > nesD_{\text{ext}}/d$, where $D_{\text{ext}} \propto H^{-1}$ is the extreme diameter of the cyclotron orbit of an electron and d is the thickness of the sample and is associated with longitudinal phonon generation in the skin layer with thickness $\sim D_{\text{ext}}/2$, provided that a static skin-effect occurs.[9] In 1993 a similar effect[10] was found in a massive ($d=0.1$ cm) single-crystal Bi sample in zero magnetic field. This kink can be attributed to the anomalous skin effect, where longitudinal phonons are generated in the skin layer with thickness δ when $j > (nes)\delta/l$, where $l \gg \delta$ is the mean free path of the electron.

In the aforementioned studies, the acoustoelectric nonlinear properties of Bi were investigated by measuring the longitudinal-voltage component. In this work we show that very fruitful information may be obtained by studying the transverse voltage in the phonon-generation mode. The first attempt of this kind was undertaken with inhomogeneous Bi samples[11] in which some regions have a short mean free path $l \sim v_f/\Omega$, where v_f is the Fermi velocity and $\Omega \approx 10^{13}$ Hz.

In what follows, we present the results of the systematic study of the transverse-voltage $V_\perp$ in a homogeneous, high-purity Bi sample in the phonon-generation regime

subject to strong crossed electric and magnetic fields. We have developed a method of extracting the acousto emf $\mathbf{E}^a$ from the transverse-voltage data. The acousto emf at $v_\perp^d \geq s$ is a measure of phonon generation and is expressed as[12,13,6]

$$\langle \partial \mathbf{P}/\partial t \rangle = -ne\mathbf{E}^a , \quad (1)$$

where $\langle \partial \mathbf{P}/\partial t \rangle$ is the average change in momentum of the electronic system per unit time. $\mathbf{E}^a$ was measured directly by means of the I-$V_\perp$ curves and it was found that $V_\perp(I)$ exhibits a negative differential conductivity at $j > j_k$ and an inversion of sign as the current is swept upwards. The absolute value of the nonlinear transverse voltage is extremely sensitive to the reversal of the direction of the current or the magnetic field.

Similar nonreciprocity effects were observed earlier for the longitudinal voltage when the current direction was reversed.[6] This phenomenon can be associated with the fact that nonequilibrium phonons are damped at the transverse sample boundaries and this damping is critically dependent of the particular structural defects on each boundary. Furthermore, in Bi there may be a component of $V_\perp$ that is even in the magnetic field. The even component arises from the tilt of the electron Fermi-surface quasiellipsoids with respect to the basal plane. This, in combination with the odd component, can lead to a phonon flux that takes on different absolute values when $\mathbf{H}$ is inverted.

In the present study, several transient effects found in longitudinal-voltage studies[5-7] have been found. They are electroacoustic oscillations of nonlinear response, the dependence on magnetic field of the relaxation time characterizing the transition to the nonlinear regime, and the so-called "aftersound." Aftersound, a term used in electroacoustics, arises when an applied electric field, large enough to put the system in the nonlinear, phonon-generation regime, is abruptly switched off. Nonequilibrium phonons continue to drag the electrons for some time after the field is switched off, giving rise to a residual voltage.

We further found that under certain conditions electroacoustic oscillations were transformed into noise. This result reveals the presence of acoustic turbulence and a transition to chaos. It was shown experimentally that the absolute value of the voltage "overfall" (defined as the difference between the measured voltage in the nonlinear region of the I-$V_\perp$ curve and the kink voltage) increases until, at some very high current value, it begins to decrease. This gives rise to an S-shaped I-$V_\perp$ curve (see Fig. 4). This feature can be attributed to an increase on phonon-phonon damping as the current increases, i.e., the coefficient in the phonon kinetic equations responsible for this mechanism increases. This brings about a reduction in the acousto emf.

EXPERIMENT

We studied a 99.9999% pure single crystal of Bi with dimensions $1\times1\times6$ mm^3. The longitudinal axis is parallel to bisectrix direction $C_1 \| y$. The transverse faces coincide with the directions $C_2 \| x$ (the binary crystallographic axis) and $C_3 \| z$ (the trigonal crystallographic axis). The measurements were done at 4.2 K. The contacts for the transverse-voltage measurements were made on opposite faces perpendicular to C_2. The magnetic-field vector lies in the C_2-C_3 plane 5° from the C_3 axis. The longitudinal voltage was measured by use of current leads placed in C_2C_3 planes.

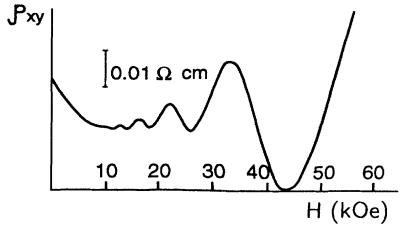

FIG. 1. Shubnikov–de Haas oscillations of the nondiagonal component of magnetoresistance tensor.

The quality of the sample was estimated from the ratio of the sample resistance measured at room temperature to its value at 4.2 K in zero magnetic field as well as from the amplitude of Shubnikov–de Haas oscillations. These parameters were measured using a Keithley 224 dc current source. The value of $R_o^{300\,\mathrm{K}}/R_o^{4.2\,\mathrm{K}}$ was found to be 190. Subnikov–de Haas oscillations as measured at 10 mA are shown in Fig. 1. The oscillations are monofrequent in H^{-1} and have a rather large amplitude of about 10% with respect to the monotonic part of the magnetoresistance along C_1. The period of the oscillations $\Delta(H^{-1}) = 1.56\times10^{-5}$ Oe^{-1} corresponds to the maximum cross section of the hole Fermi surface.[14] Inversion of the magnetic field shifts the phase of the oscillations by π. At H=56 kOe, the ratio $V_\perp(+\mathbf{H})/V_\perp(-\mathbf{H}) = \rho_{xy}(+\mathbf{H})/\rho_{xy}(-\mathbf{H}) = -2, \phi\rho_{xy}(+\mathbf{H}) = 0.183$ Ω cm, and $\rho_{yy} = 0.3$ Ω cm, where ρ_{ik} are the components of the general magnetoresistivity tensor.

The properties of the sample in the phonon-generation regime were studied using a 45-V-peak pulse with a pulse duration of $\cong 4.3$ μs and a duty cycle of 0.1 s. A pulsed-current method was chosen so that sample heating effects would be negligible. The sample was connected as a load to the pulse generator in series with a reference resistor $R_N = 1$ Ω. (The lead resistance was about 0.3 Ω.) The current was measured by monitoring the voltage drop across the reference resistor.

Figures 2(a)–2(c) shows the time dependence of the transverse sample voltage in a magnetic field of 52.3 kOe with three different configurations of field and current direction. Figure 2(d) shows the voltage across the reference resistor, i.e, the current pulse. We assume that the transition to the nonlinear regime takes place when $\partial V_\perp/\partial t = 0$. (This is also when $\partial V_\perp/\partial I = 0$ since the current is increasing monotonically at this point.) Noting that the kink in the I-$V_\perp$ curves occurs at nearly the same value of current I_k for both the transverse and longitudinal voltages and using the longitudinal voltage corresponding to this kink to estimate the drift velocity, we find that $v_\perp^d \cong cE/H \cong 1.1\times10^5$ cm/s. Since this value is

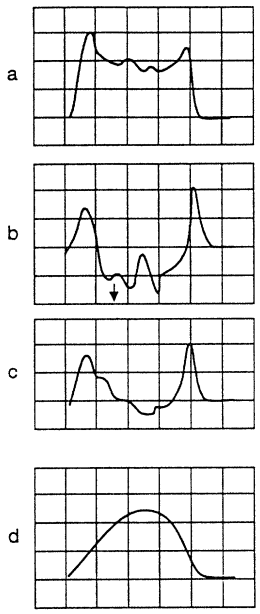

FIG. 2. Oscillograms of $V_\perp(t)$ (a)–(c) and $I(t) \propto V_{RN}$ (d) signals, $H = 53.2$ kOe. Horizontal scale: 1 μs/div. Vertical scale: (a)–(c) 1 V/div, (d) 2 V/div. Magnetic field and current orientations: (a) $+\mathbf{H}, +\mathbf{I}$; (b) $-\mathbf{H}, +\mathbf{I}$; (c) $-\mathbf{H}, -\mathbf{I}$. "Zero" of the each trace coincides with the horizontal line at the end of the pulse.

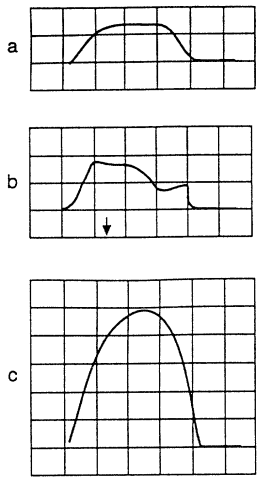

FIG. 3. Oscillograms of $V_\perp(t)$ (a) and (b) and $I(t) \propto V_{RN}$ (c) signals, $H = 14.94$ kOe. Horizontal scale: 1 μs/div. Vertical scale: (a) 1 V/div, (b) 0.5 V/div, (c) 2 V/div. Magnetic field and current orientations: (a) $+\mathbf{H}, +\mathbf{I}$; (b) $-\mathbf{H}, +\mathbf{I}$.

approximately equal to s and given the results of previous work,[2–6] we can conclude that the observed transition to nonlinear behavior is due to phonon generation.

The main observed properties of the transverse voltage can be summarized as follows.

(1) The value of the transverse voltage in the nonlinear regime strongly depends on the directions of magnetic field and current ($\pm\mathbf{H}, \pm\mathbf{I}$). The voltage overfall reaches a maximum for direction $-\mathbf{H}$ and $+\mathbf{I}$ [Fig. 2(b)]. Moreover, the transverse voltage actually changes sign for configurations $-\mathbf{H}, +\mathbf{I}$ and $-\mathbf{H}, -\mathbf{I}$ [Figs. 2(b) and 2(c)]. For all configurations of current and field directions, a negative differential resistance was observed (Figs. 2 and 4).

(2) The current at which the transition to the nonlinear regime occurs, I_k^+, (as well as the current at which linearity is restored as the current ramped down, I_k^-) is larger for $+\mathbf{H}$ than for $-\mathbf{H}$ (Fig. 2 and Fig. 4—see dashed line). The same conclusion can be reached from the data in Fig. 3. The current dependence of transverse voltage is nearly linear at a magnetic field of 14.94 kOe for the direction $+\mathbf{H}$ and clearly nonlinear for the $-\mathbf{H}$ direction at corresponding values of current. Similarly, as the current direction is switched from $+\mathbf{I}$ to $-\mathbf{I}$, both I_k^+ and I_k^- increase. [Figs. 2(b) and 2(c)].

(3) For the configuration $-\mathbf{H}, +\mathbf{I}$ (and to a lesser extent for $-\mathbf{H}, -\mathbf{I}$) the absolute value of the transverse voltage is smaller for the transition to the nonlinear regime (as measured by the maximum voltage as the current is increased) than for the back transition (as measured by the maximum as the current is decreased). In these configurations, $\mathbf{I}_k^+$ is larger than $\mathbf{I}_k^-$ (Fig. 2).

(4) Electroacoustic oscillations of $V_\perp$ have maximum amplitude for the configuration $-\mathbf{H}, +\mathbf{I}$ (Fig. 2). These oscillations can be seen in the dynamical I-$V_\perp$ curves, where $V_\perp$ fluctuates about its average (static) value. (Fig 4, curves 1 and 2.) A dynamic I-$V_\perp$ curve is one that is derived by comparing corresponding values from the time-dependent current and voltage signals.

(5) The time interval from the transition to the nonlinear regime to when $V_\perp$ reaches a minimum is about 2 μs at $H = 14.94$ kOe. This rather long relaxation time results in the asymmetrical shape of the transverse-voltage signal with respect to the peak in the current pulse. [Figs. 3(b) and 3(c)]. When $H = 52.3$ kOe, the relaxation time can be estimated from noting the appearance of a sudden change in the slope of $V_\perp$ as a function of time. At this point, we believe that the system enters the stationary state (see Fig. 6 and caption). This method of estimating the relaxation time is commonly applied in longitudinal-voltage studies.[5,6] As can be seen in Figs. 2(a) and 2(b), $V_\perp(t)$ exhibits a large negative slope immediately after entering the nonlinear regime; the curve then rapidly flattens out in a time $\tau_r \approx 0.5$ μs, as measured from when the voltage first reaches a maximum. This is in agreement with longitudinal-voltage studies.[6]

(6) When $H = 29.9$ kOe and for the configuration $-\mathbf{H}, +\mathbf{I}$, two points are observed where $dV_\perp/dI = 0$. (See Fig. 4, curve 3.) The first, at $I \cong 2.6$ A, corresponds to the transition to the nonlinear regime. The second occurs at $I \cong 6$ A. At this point, the charge drift velocity $\mathbf{v}_\perp^d \cong cE/H$ is estimated to be about 2×10^5 cm/s.

Let us conclude this section by noting that the data in this study are not degraded by heating effects. In the linear regime the values of $\rho_{xy}(\pm\mathbf{H}, \pm\mathbf{I})$ measured with a pulsed current agree within experimental error with the results of dc measurements with $I = 10$ mA. This indicates that the sample temperature change during the

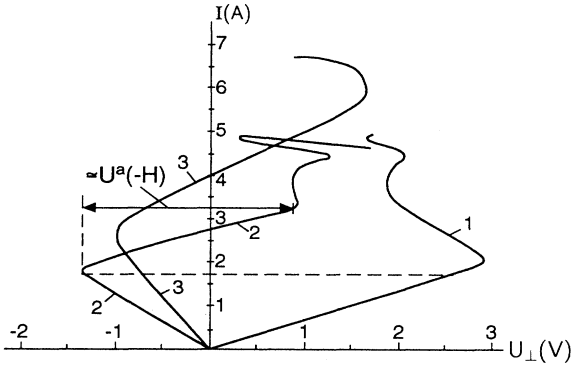

FIG. 4. I-$V_\perp$ curves for $H=52.3$ kOe (1,2) and $H=29.9$ kOe (3). Magnetic field and current orientation are 1, $+\mathbf{H},+\mathbf{I}$; 2, $-\mathbf{H},+\mathbf{I}$; 3, $-\mathbf{H},+\mathbf{I}$.

current pulse is negligible. Thermal effects could be uncovered by gradually decreasing the duty cycle and noting that the slope of the nonlinear part of the I-$V_\perp$ curve decreases towards the linear value.

DISCUSSION

Let us assume that in the phonon-generation regime the average change in momentum of the electron and phonon subsystems per unit time are equal. In this case [see Eq. (1)]

$$\langle \partial \mathbf{P}/\partial t \rangle_e = -\langle \partial \mathbf{P}/\partial t \rangle_p = -\bar{\mathbf{q}} \sum_{\mathbf{q}} \hbar q \langle \partial N_{\mathbf{q}}/\partial t \rangle = -ne\mathbf{E}^a \ . \tag{2}$$

Hence,

$$\mathbf{E}^a = \bar{\mathbf{q}} \langle \partial \epsilon/\partial t \rangle_p / nes \ , \tag{3}$$

where $\langle \partial \epsilon/\partial t \rangle_p = \sum_{\mathbf{q}} \hbar s q \langle \partial N_{\mathbf{q}}/\partial t \rangle$ and $\bar{\mathbf{q}}$ is the unit vector.

The condition for phonon generation is $\mathbf{q}\cdot\mathbf{v}^d \geq \omega$, where ω is the phonon frequency. This means that phonons are emitted into a Cherenkov-type cone. The direction of the net recoil momentum is on average opposite to the drift velocity; this implies that $\mathbf{E}^a$ is parallel to $\mathbf{v}^d$. In strong crossed electric and magnetic fields $\mathbf{v}_\perp^d/\mathbf{v}_y^d \sim \Omega t \gg 1$ and, therefore, we can assume that $\mathbf{v}_\perp^d \cong \mathbf{v}^d$.

Let us express the phonon distribution function as a sum of equilibrium ($N_{\mathbf{q}0}$) and nonequilibrium ($N_{\mathbf{q}}^{(1)}$) terms. This yields

$$\mathbf{E}^a \propto \sum_{\mathbf{q}} \langle \partial N_{\mathbf{q}}/\partial t \rangle = \sum_{\mathbf{q}} \alpha_{\mathbf{q}} (N_{\mathbf{q}0} + N_{\mathbf{q}}^{(1)}) + \alpha_{\mathbf{q}}^f \ , \tag{4}$$

i.e., the acousto emf is determined by the number of phonons in the stationary state, the growth coefficient $\alpha_{\mathbf{q}}$, and the interaction of charge carriers with the zero-point lattice vibrations, indicated by $\alpha_{\mathbf{q}}^f$.

Let us assume $\alpha_{\mathbf{q}} N_{\mathbf{q}} \gg \alpha_{\mathbf{q}}^f$ and $\alpha_{\mathbf{q}}$ are almost independent of temperature (the effective Debye temperature in Bi is $\Theta_D^* \sim 1-10$ K). The effective Debye temperature, usually used in the description of semiconductors, is determined from the relation $\Theta_D^* = s\hbar q/k_B$, where $\hbar q = p_f$, the Fermi momentum. When $\hbar q > p_f$, energy is no longer conserved. In Bi, electrons can effectively interact with phonons of momentum less than $(0.5-7)\times 10^{-21}$ g sm/s. The limits of this range corresponds respectively to the minor and major axes of the electron Fermi-quasi-ellipsoids.[14] Thus, $\Theta_D^* \sim 1-10$ K. In this case, if we take $N_{\mathbf{q}}^{(1)}=0$, which is equivalent to Miyake and Kubo's[15] assumption of an equilibrium phonon-distribution function, the acousto emf should increase with temperature. On the contrary, for $N_{\mathbf{q}}^{(1)} \gg N_{\mathbf{q}0}$, an increase in temperature will result in a considerable reduction of the acousto emf due to the scattering of nonequilibrium phonons off of thermal ones. Since previous work[6] indicates that the acousto emf in Bi decreases significantly as temperature increases (in the range 4.2–20 K), we conclude that the phonon distribution is nonequilibrium in this study. We believe this explains why the experimental data is inconsistent with some theoretical predictions.[15]

Introducing a coefficient γ as the fraction of input electric power W that is transformed into acoustic flux, the acousto emf may be expressed, neglecting equilibrium and zero-point vibration amplification, as[6]

$$\mathbf{E}^a \cong (\gamma-\beta) W/nes \ , \tag{5}$$

where β describes sound damping.

In Bi, the contribution to the phonon flux from supersonic electrons is much larger than that from holes. This claim is supported by both the ratio of the deformation potential constants for electrons and holes[16] as well as by experimental data.[7] Moreover, it was shown earlier[6] when $\mathbf{I} \| C_1, \mathbf{H}$ is in the C_2-C_3 plane ($\langle H, C_3 \approx 10°$), the hole drift velocity is $(v_\perp^d)_h \cong cE/H$ and its direction is close to the binary axis. The drift velocity for an electron in one of the electron quasiellipsoids is approximately $(v_\perp^d)_e \cong 2cE/H$ and is directed at an angle of about 45° from the trigonal axis in the C_2-C_3 plane. (The drift velocity values were determined from the components of the mobility tensor.[17]) Longitudinal and two shear acoustic mode velocities along the binary axis are, respectively, 2.54×10^5, 1.55×10^5, and 0.85×10^5 cm/s. Because of bismuth's crystalline symmetry, deformation interaction between charge carriers and transverse phonons moving along C_2 is rather small. So, given the present experimental geometry, phonon generation by holes is appreciable only when $cE/H > 2.5\times 10^5$ cm/s.

The transverse magnetoconductance has a part that is an even function of magnetic field. We may write this component for small angle θ (see Fig. 5) as[19]

$$\sigma_{xy}^{\text{even}} \cong nec^2(\mu_{xx}-\mu_{yy})\mu_{xx}\mu_{yz}H_xH_z/\mu_{xx}^2\mu_{yy}^2H_z^4 \ , \tag{6}$$

where μ_{ik} are the components of the electron mobility tensor.

Assuming that $\mu_{ik} \to \mu_e^0$ and $\mu_{xx}-\mu_{yy} \sim \mu_e^0$, it is easy to obtain

$$\sigma_{xy}^{\text{even}}(\pm\mathbf{H}) \cong -(nec/H)\sin\theta(\mu_e^0 H/c)^{-1} \ . \tag{7}$$

Introducing $\Delta n = n_e - n_h$, the difference in electron and

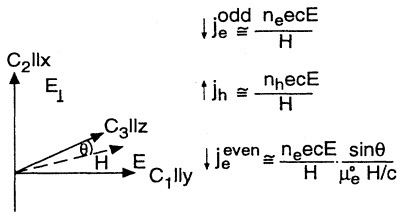

FIG. 5. Scheme of experiment.

hole concentrations, we get $\sigma_{xy}^{odd} \cong -\Delta nec/H$, and hence

$$\sigma_{xy}(\pm\mathbf{H}) \cong \mp(nec/H)[\Delta n/n \pm \sin\theta(\mu_e^0 H/c)^{-1}] . \quad (8)$$

This gives $|\sigma_{xy}(+\mathbf{H})/\sigma_{xy}(-\mathbf{H})| > 1$, which agrees with our experimental results.

Assuming that $\rho_{xy}/\rho_{yy} \sim (\Delta n/n)\Omega\tau$, $\Omega\tau \sim \mu_e^0 H/c \sim 10^3$ we estimate that $\Delta n/n \sim 10^{-3}$. Since experimentally $\sigma_{xy}(+\mathbf{H})/\sigma_{xy}(-\mathbf{H}) \cong \rho_{xy}(+\mathbf{H})/\rho_{xy}(-\mathbf{H}) = -2$, we find that $|\sigma_{xy}^{odd}/\sigma_{xy}^{even}| \cong 3$. On the other hand, we can determine the same ratio using Eq. (8) and the above estimates of $\Omega\tau$ and $\Delta n/n$; this gives a value of 10. Hence, Eq. (8) seems to work to within an order of magnitude.

Let us assume that the sample is infinitely long in the z direction and consider the acousto emf of electrons drifting in the x direction. Imposing the condition that no current flow in the x direction and neglecting diffusion effects, the transverse-voltage $V_\perp$ in the phonon-generation regime may be written as

$$E_\perp(\pm\mathbf{H}) \cong \pm(nec/H)[\Delta n/n \pm \sin\theta(\mu_e^0 H/c)^{-1}] \times E(n_e e\mu_e^H + n_h e\mu_h^H)^{-1} \mp E^a , \quad (9)$$

where $\mu_{e,h}^H \sim \mu_{e,h}^0/(\Omega_{e,h}\tau_{e,h})^2$ are the mean electron and hole mobilities in the x direction, $E^a \propto jE$ [see Eq. (5)] and $n_e e\mu_e^H \geq n_h e\mu_h^H$.

Figure 6 schematically shows a rectangular longitudinal-voltage driving pulse with $E > Hs/c$. It also shows the current I and transverse-voltage $V_\perp$ pulses on the sample. The I and $V_\perp$ signals reach stationary values after a time τ_r, the relaxation time for entry into the phonon-generation regime. When the driving pulse is sufficient to put the system into the phonon-generation regime, the conductivity increases, resulting in a decrease in the measured transverse voltage. The vertical arrow in Fig. 6 indicates the acousto emf, the difference between the value of the transverse voltage at $t < \tau_r$ and its value at $t > \tau_r$. This brings about a negative differential conductance in the I-$V_\perp$ curve. According to Eq. (9), a reversal of the sign of $V_\perp$ is most likely to occur when the magnetic field is in the $-\mathbf{H}$ direction. All of these features are indeed observed experimentally (Figs. 2 and 4).

The longitudinal voltage grows by $\simeq 30\%$ after the system relaxes into the phonon-generation regime until current reaches the maximum value I_{max} for $H = 52.3$ kOe. This explains why the value of the acousto emf $E^a \cong 25$ V/cm ($E^a/E \cong 0.4$), derived from Eq. (9) [where $E_\perp(\pm\mathbf{H})$ and the first term on the right-hand side are, respectively, the nonlinear and linear experimental fields]

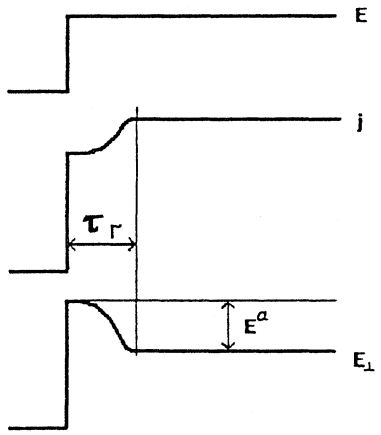

FIG. 6. Experimental setup for acousto emf measurements.

seems to be slightly low (see Fig. 4, curve 2). As mentioned above, the accuracy of Eqs. (6)–(9) is within an order of magnitude. Evaluating the acousto emf using Eq. (5) with $\gamma = 1$ and $\beta = 0$ and using experimental data for the longitudinal voltage and current gives $E^a \cong 6.5$ V/cm.

We can see from Figs. 2(b) and 2(c) that under present experimental conditions a reversal of the current direction ($+\mathbf{I} \rightarrow -\mathbf{I}$) results in a decrease in the acousto emf to $\cong 20$ V/cm when the magnetic field is in the $-\mathbf{H}$ direction. In Ref. 6, the effect of reversing the direction of the drift velocity on the longitudinal voltage is discussed. Following that discussion, we believe that the change in the acousto emf ΔE^a when the direction of current is reversed can be explained by the fact that the nonequilibrium phonons experience different degrees of damping on the opposite faces of the sample, most likely because each face has unique structural defects [$\Delta E^a \sim (W/nes)\Delta\beta$].

According to Figs. 2 and 4, when the magnetic field is reversed ($-\mathbf{H} \rightarrow +\mathbf{H}$) with the current in the $+\mathbf{I}$ direction, the acousto emf decreases to $\cong 10$ V/cm. Both the magnitude and sign of the linear transverse electric field change when $\mathbf{H}$ is reversed. Using the fact that the dielectric constant of Bi is $\sim 10^2$, the linear transverse electric field $E_\perp \cong 30$ V/cm (Fig. 4, curve 1) corresponds to a surface electron density of $n_s \sim 2 \times 10^9$ cm^{-2}. (A surface charge density order 10^{10} cm^{-2} of magnitude causes the conductance band to bend near the edges of the sample by an amount of the order of the Fermi energy $\varepsilon_f \sim 10^{-14}$ erg and extends into the sample a length of about the Debye radius $r_D \sim 10^{-5}$ cm.) A change in n_s and $E_\perp$ when the direction of $\mathbf{H}$ is reversed may affect the mobile-carrier intervalley-scattering probability on the surface, resulting in a variation of the carrier-concentration gradients near the surface. [Such gradients, which arise because of the difference in the electrons (and holes) intervalley and intravalley mobilities, have a length scale of the order of the diffusion length[20] $L \sim r(\tau_i/\tau)^{1/2} \sim 10^{-4}$ cm, where r is the Larmor radius and $\tau_i \sim 10^{-8}$ s (Ref. 21) and $\tau \sim 10^{-10}$ s are, respectively, the intervalley and intravalley bulk relaxation times.] In

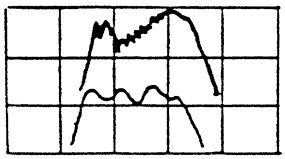

FIG. 7. Transformation of electroacoustic oscillations into noise. Sample dimensions are $1\times1\times8$ mm^3; horizontal scale is 1 μs/div; vertical scale is 1 V/div; $\mathbf{H}\|C_1;\mathbf{I}\|C_2$. Lower trace: $H=14.9$ kOe, $I_{\max}=5$ A. Upper trace: $H=22.7$ kOe, $I_{\max}=7$ A.

turn, the change in the concentration gradient should alter the magnitude of the diffusion current of electrons moving opposite to the phonon flux; that is, the phonon absorption changes. In other words, the value of β in Eq. (5) should also change, leading to a variation of the acousto emf.

The decrease in the acousto emf when we switch the direction of current ($+\mathbf{I}\rightarrow-\mathbf{I}$) and field ($-\mathbf{H}\rightarrow+\mathbf{H}$) is obviously related [see Eq. (9)] to the experimentally observed shift towards larger value of currents of the transition to the nonlinear regime (and back to the linear) (see Figs. 3 and 4, curves 1 and 2).

The amplitude of the electroacoustic oscillation decreases when the direction of both the current and magnetic field are reversed (from $-\mathbf{H},+\mathbf{I}$) (see Fig. 2). Earlier it was suggested[6] that oscillations arise from the motion of acoustoelectric domains that originate near the sample face and propagate in the Hall direction towards the opposite boundary. Under certain conditions monochromatic electroacoustic oscillations are transformed into noise. Figure 7 shows the most striking picture obtained for longitudinal-voltage measurements on a sample similar to the one used in this work. The observation of electroacoustic noise suggests the appearance of acoustic turbulence and the transition to chaos. This phenomenon requires further detailed study.

The phenomenon of "aftersound" was observed in longitudinal-voltage studies.[5,7] A similar effect was found during measurements of the transverse voltage in the present study [Figs. 2(b) and 2(c)]. This effect is revealed by the fact that the voltage peak that corresponds to reentry into the linear regime (at I_k^-) is larger than the one that corresponds entry into the nonlinear regime (at I_k^+). This can be explained by the dragging of the electrons by excited nonequilibrium phonons, producing an additional voltage drop. The time scale for this effect should be of the order of the phonon-electron relaxation time τ_{pe}. In our experiment $\tau_{pe}\geq0.3$ μs. Assuming the acoustic absorption coefficient to be $\alpha\cong(s\tau_{pe})^{-1}$, we can estimate $\alpha\leq30$ cm^{-1}, consistent with the data taken[22] at frequency $\omega\cong10^9$ s^{-1}, $H\cong10$ kOe, and $T=4.2$ K.

The aftersound emf value E_p, defined as the difference in magnitude of the voltage peaks on front and rear edge of the pulse [Fig. 2(b)], has a rather large value of $E_p\cong7.5$ V/cm for configuration $-\mathbf{H},+\mathbf{I}$. E_p can be interpreted as the acousto emf associated with momentum transfer from phonon subsystem to the electron subsystem when $v^d<s$. The fact that E^a and E_p have close (approximately equal) values is compelling evidence of the strong phonon-electron interaction in the Bi crystal under investigation. As expected, the phonon flux decrease with the reversal of the direction of both the magnetic field and current is accompanied by the gradual vanishing of aftersound effect [Figs. 2(c) and (2a)].

If the rise time of current pulse is of the order of the relaxation time for transition to the nonlinear regime, the peak on the dynamic I-$V_\perp$ curve is shifted towards the larger values of current when compared with stationary I-$V_\perp$ curves. This transient effect can hinder the observation of aftersound, since the height and shape of the voltage peaks may depend delicately on the shape of the current pulse [Figs. 2(a) and 3(b)].

According to the analysis in Ref. 6, in crossed electric and magnetic fields the dynamics of the transition to the nonlinear regime of a finite Bi sample can be described in terms of phonon-electron interactions. Phonon-electron damping is possible and dominant when the excited acoustic wave reflects from the sample face and propagates in the direction opposite to the drift velocity of the charge carriers. In keeping with Ref. 6, the relaxation time for entering the nonlinear regime and for the transverse voltage to reach equilibrium in samples with the thickness $d>s\tau_{pe}$ is mainly determined by τ_{pe}. Since the electronic density of states increases with magnetic field, the value of τ_{pe} as well as the relaxation time τ_r decrease as H increases (Figs. 2 and 3).

As mentioned above, in a magnetic field of $H=29.9$ kOe ($-\mathbf{H}$ direction) at $I>6$ A the absolute value of the voltage overfall decreases as the current is swept up. This can be attributed to the fact that the acousto emf decreases as the current rises (Fig. 4, curve 3). This feature could be explained by the generation of phonons by supersonic holes, whose acousto emf is opposite in sign to that of the electrons. However, within the present experimental geometry, the hole drift velocity is probably not enough for the excitation of the longitudinal-acoustic mode (see above). Another possible explanation is the dependence of the coefficient that defines nonlinear phonon-phonon damping ($-\beta^d N_q^2$) in the kinetic equation for phonons.[7] It is evident that if β^d as a function of drift velocity increases faster than α_q, then the nonequilibrium-phonon concentration $N_q^{(1)'}\sim\alpha_q/\beta^d$ will decrease, leading to a reduction of the acousto emf. The physical reason β^d increases as a function of drift velocity is due to the expansion of the Cherenkov radiation cone:[13] $\beta^d\sim1-s/v^d$.

The decreasing voltage overall is not observed for the magnetic field oriented in the $+\mathbf{H}$ direction, probably due to the relatively small phonon flux magnitude.

It should be noted that a similar phenomenon was found in the study[7] of longitudinal phonon generation in the bulk of filamentous crystals of Bi at $H=0$ and was explained there in terms of the fact that β^d is an increasing function of v^d. This phenomenon appears as an abrupt change in the slope of the I-V curve at $j/j_k\sim10$, followed by a regime of increased conductivity. Using a

phenomenological description of the I-V curves, namely $j=\sigma(E-E^a)$, this second kink observed in Ref. 7 may be formally interpreted as a decrease in the acousto emf.

In summary, if the electron drift velocity is high enough, the nonlinear phonon-phonon interaction is believed to play a dominant role in stabilization of the acoustic instability that occurs in the presence of crossed electric and magnetic fields. All earlier attempts to observe the influence of the nonlinear phonon-phonon interactions on the I-V curves in the phonon-generation regime at $\mathbf{E}\perp\mathbf{H}$ and $d>s\tau_{pe}$ probed the longitudinal voltage and, hence, were unsuccessful.

Sound generation in Bi was found many years ago. However, existing theory has only been able to describe the initial part of the acoustoelectric instability corresponding to the slightly nonequilibrium distribution function. Comparing experiment with theory[15,23–27] (we do not refer to phenomenological models), one has only the qualitatively conclusion that supersonic carrier drift velocities in Bi are related to the amplification and generation of elastic waves.[2,3–8,8–11,22] It is quite evident that concerted theoretical attention to the study of highly nonequilibrium states, which are affected by complex interactions between quasiparticles and collective excitations, is needed to generate theories that agree quantitatively with experimental results.

[1]A. R. Huston, J. H. McFee, and D. L. White, Phys. Rev. Lett. **7**, 237 (1961).

[2]A. M. Toxen and S. Tansal, Phys. Rev. Lett. **10**, 481 (1963).

[3]L. Esaki, Phys. Rev. Lett. **8**, 4 (1962).

[4]K. Walther, Phys. Rev. Lett. **16**, 642 (1965).

[5]T. Jamada, J. Phys. Soc. Jpn. **20**, 1647 (1965).

[6]Yu. A. Bogod, Fiz. Nizk. Temp. **8**, 787 (1982) [Sov. J. Low Temp. Phys. **8**, 393 (1982)].

[7]Yu. A. Bogod, D. V. Gitzu, and A. D. Grozav, Zh. Eksp. Teor. Fiz. **84**, 2194 (1983) [Sov. Phys. JETP **57**, 1279 (1983)].

[8]Yu. A. Bogod, D. V. Gitzu, and A. D. Grozav, Zh. Eksp. Teor. Fiz. **90**, 1010 (1986) [Sov. Phys. JETP **63**, 1279 (1986)].

[9]M. Ya. Azbel, Zh. Eksp. Teor. Fiz. **44**, 983 (1963) [Sov. Phys. JETP **17**, 667 (1963)].

[10]Yu. A. Bogod, Solid State Commun. **87**, 1159 (1993).

[11]S. V. Bengus, Yu. A. Bogod, and P. E. Finkel', Fiz. Nizk. Temp. **16**, 738 (1990) [Sov. J. Low Temp. Phys. **16**, 434 (1990)].

[12]A. Weinreich, Phys. Rev. **107**, 317 (1957).

[13]H. Ozaki and N. Mikoshiba, J. Phys. Soc. Jpn. **21**, 2486 (1966).

[14]V. S. Edel'man, Usp. Fiz. Nauk **123**, 257 (1977) [Sov. Phys. Usp. **20**, 819 (1977)].

[15]S. J. Miyake and R. Kubo, Phys. Rev. Lett. **9**, 62 (1962).

[16]K. Walther, Phys. Rev. **174**, 782 (1968).

[17]R. Hartman, Phys. Rev. **181**, 1070 (1969).

[18]Y. Eckstein, A. W. Lawson, and D. H. Reneker, J. Appl. Phys. **31**, 1534 (1960).

[19]J. E. Aubrey, J. Phys. F **1**, 493 (1971).

[20]G. I. Babkin and V. Ya. Kravchenko, Zh. Eksp. Teor. Fiz. **60**, 695 (1971) [Sov. Phys. JETP **33**, 378 (1971)].

[21]A. A. Lopez, Phys. Rev. **175**, 823 (1968).

[22]K. Walther, Phys. Rev. Lett. **15**, 706 (1965).

[23]R. F. Kazarinov and V. G. Scobov, Zh. Eksp. Teor. Fiz. **43**, 1492 (1962) [Sov. Phys. JETP **16**, 1057 (1963)].

[24]W. P. Dumke and R. R. Hearing, Phys. Rev. **126**, 1974 (1962).

[25]A. A. Vedenov and E. P. Velikhov, Zh. Eksp. Teor. Fiz. **43**, 1110 (1962) [Sov. Phys. JETP **16**, 784 (1963)].

[26]A. A. Grinberg, Fiz. Tverd. Tela (Leningrad) **6**, 911 (1964) [Sov. Phys. Solid State **6**, 701 (1964)].

[27]V. P. Kalashnikov, Fiz. Met. Metalloved. **16**, 19 (1963).